International Journal of Applied Engineering Research ISSN 0973-4562 Volume 12, Number 19 (2017) pp. 9159-9166

Effect of Baffles Geometry on Hydrodynamics in a Mechanically Agitated System

L. Benyamina[1], M. Bouanini[2] and R. Abdeldjebar[3]

[1]PhD in Physics Energetics, [2]Doctor in Energy Physics, [3]Magister Energy Physics
[1,2,3] Bechar university , BP417 Route de Kenadza, Bechar 08000, Algeria.

ORCID IDs: [1]0000-0001-8108-7328, [2]0000-0002-9657-3422, [3]0000-0002-7606-2895

Abstract

Mechanically agitated systems are at the heart of many manufacturing processes. Without them, few chemical reactions or mixtures would occur. In these systems the agitator can be subjected to high stresses (radial force, axial force, pressure prevailing in the tank, vibratory phenomena ...), for this, a study is conducted where baffles are placed at level and this to break the vortices which are at the origin of the vibrations which can lead to the wear and the damage of the agitators, and thus to brake the tangential flow (in block), and in order to create the radial and axial flow, So it is a 2D hydrodynamic study aimed at designing the effect of baffle geometry on turbulent flow and their impact on system energy consumption and mixing homogeneity. CFD Fluent software package was used and the multiple references frame and the rotating domain techniques are applied to simulate the behavior of flow pattern inside the stirred.

Keywords: Baffles Geometry, Turbulent Flow, Hydrodynamics, Rotating Domain, CFD

INTRODUCTION

Mixing is an important unit operation in many technologies, involved in food, pharmaceuticals, polymers industries [1-7, 8] by reducing the non-uniformities or gradients in composition, physical properties of the materials in and outside of a reactor. A good mixing produces a uniform mixture with a low operating cost and time. Turbulent mixing is typically carried out in baffled tanks, which are usually equipped with four equally-spaced baffles with the width of the baffle usually being one-twelfth to on tenth of the tank diameter.[9] In these tanks, power consumption increases with the number of baffles, but a decrease in the number of baffles results in poor mixing. Without baffles, swirl and central vortex formation may be experimented, which results inflow shear rate, even if a high shear impeller, like the Rushton turbine, is used. Baffles change the flow patterns by converting part of the circumferential and radial velocity components into the axial velocity component.[10,17] This enhances the axial circulation of the fluid, and at the same time introduces loops in the vicinity of the baffles. These loops can be suppressed by an increased upward current induced by a draft tube. The optimum design and the efficiency of mixing operations are important parameters on product quality and production costs. The flow motion and in stirred tanks is 3-dimmensional and complex. In the area surrounding the impeller, the flow is highly turbulent and swirling [18 the CFD study using different turbulence models like, k – ε, RNG k – ε and RSM for the prediction of tangential velocity distribution in a baffled vessel using multiple reference frames (MRF) model[19]. The turbulent flow field generated in baffled stirred tank was computed by large eddy simulation (LED) and the flow field was developed using the Sliding Mesh (SM) approach. Mixing times and power number have been determined for a vessel agitated by a 6-blade Rushton turbine. The predicted results were compared with the published experimental data. [20]. The effect of the width and the length of baffle on mixing process was investigated by several researchers [21]. CFD simulations, using a gas/liquid inhomogeneous model, coupled with a homogenous turbulence model in a full transient scheme, have been run to predict the vortex shape and the flow field in an under-baffled agitated vessel during stopping the transient hydrodynamics and the free surface shape have been numerically predicted by CFD for an under-baffled agitated vessel during the stopping phase of the agitator, including the inertial period after the agitator has completely stopped. [22]The three components of mean and fluctuation velocity have been measured in a fully baffled, turbine agitated vessel with an LDV. The accuracy of measurements was confirmed by checking the volume flow rate balance around the impeller. In this study the shape of baffles in an agitated vessel are investigated numerically. [23] the effect study of the blade attack angle on the roll and training vortex structures in a stirred vessel via laser-Doppler velocimetry (LDV). In this investigation, four-bladed paddle impellers with four attack angles, which were 45◦, 60◦, 75◦and 90◦The flow produced by a flat paddle impeller (_ = 90◦) has no trailing vortex, but a pair of roll vortices.

THE GEOMETRIC MODEL

Our geometric model consist of four tanks, each equipped with four baffles of different shapes (square, circular, rectangular and trapezoidal) while having the same surface, the tank is stirred by a four-blades impeller , the system is simulated by the method of Rotating domain, The dimensions are shown in the table below:

Table 1: The Dimensions of the Geometric Model

(D) (m)	(DRD) (m)	(d)(m)	(ds) (m)	Surface of Baffles (Sb)(m^2)	(Tb)(m)
0.49	0.17	0.245	0.03	0.0009	0.009

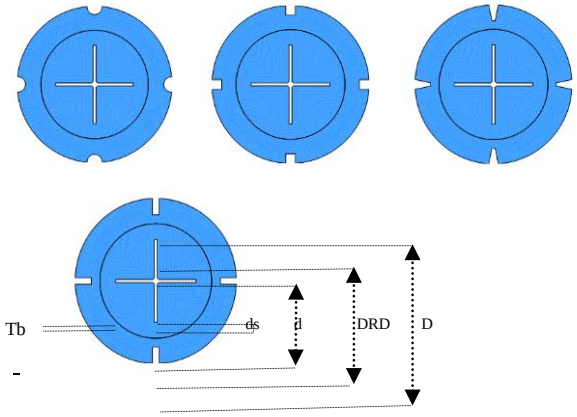

Figure 1: Modéle mathématique

THE MATHEMATICAL MODEL

A 2D study of a flux generated by a four-blade impeller with tangential flow in a cylindrical vessel was undertaken. The standard k-ε turbulent model has been chosen for numerical simulation

A Cartesian coordinate system was used, with origin located at the center of the stirrer at height H = 0, the angular position θ = 0 coincided with one of the blades of the mobile. A fluid with constant density in turbulent motion, in the Cartesian coordinates X; And Y,see Fig.2

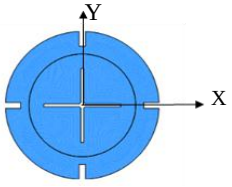

Figure 2: Cartesian coordinates model

The equations governing the flow are represented by equations which express the conservation of the mass, of the quantity Of the movement , the turbulent kinetic energy (Tke) and of the turbulent dissipation (ε).

The equations for Tke and ε, associated with the constraint relation of the viscosity, constitute the turbulence model k-ε. The (simplified) model equation for k after the use of the Boussinesq hypothesis by which the fluctuation terms can be related to the mean flux is as follows

$$\frac{\partial k}{\partial t}+\overline{U_i}\frac{\partial k}{\partial x_i}=\nu_t\left[\frac{\partial \overline{U_j}}{\partial x_i}+\frac{\partial \overline{U_i}}{\partial x_j}\right]\frac{\partial \overline{U_j}}{\partial x_i}+\frac{\partial}{\partial x_i}\frac{\nu_t}{\sigma_k}\frac{\partial k}{\partial x_i}-\varepsilon+\nu\frac{\partial^2 k}{\partial x_i \partial x_i}$$

$$with\quad \nu_t \cong 0.09\frac{k^2}{\varepsilon} \qquad (1)$$

Equation for ε

$$\frac{D\varepsilon}{Dt}=D_\varepsilon^\nu+D_\varepsilon^f+D_\varepsilon^p+P_\varepsilon^1+P_\varepsilon^2+P_\varepsilon^3+P_\varepsilon^4-Y \qquad (2)$$

where

D_ε^ν = Diffusive viscous transport

D_ε^f = Diffusive transport by fluctuation

D_ε^p = Diffusive transport by pressure fluctuation

P_ε^1 = Production by deformation of mean flow field

P_ε^2 = Production by deformation of mean flow field

P_ε^3 = Production by gradient of mean vorticity

P_ε^4 = Production by vortexstretching

Y = Viscous destruction

$$\frac{D\varepsilon}{Dt}=\frac{\partial}{\partial x_k}\left(\nu\frac{\partial \varepsilon}{\partial x_k}\right)+\frac{\partial}{\partial x_k}\left(-\overline{u'_k\varepsilon}\right)+\frac{\partial}{\partial x_k}\left(-\frac{2\nu}{\rho}\overline{\frac{\partial p'}{\partial x_i}\frac{\partial u_k'}{\partial x_i}}\right) \qquad (3)$$

$\Downarrow D^{V}\varepsilon \qquad \Downarrow D^{f}\varepsilon \qquad \Downarrow D^{p}\varepsilon$

$$-2\nu\left(\overline{\frac{\partial u'_i}{\partial x_l}\frac{\partial u'_k}{\partial x_l}}+\overline{\frac{\partial u'_l}{\partial x_i}\frac{\partial u'_{kl}}{\partial x_k}}\right)\frac{\partial \overline{U_i}}{\partial x_k}-2\nu\overline{u'_k\frac{\partial u'_i}{\partial x_l}}\frac{\partial^2 U_i}{\partial x_k \partial x_l}-2\nu\overline{\frac{\partial u'_k}{\partial x_k}\frac{\partial u'_i}{\partial x_l}\frac{\partial u'_k}{\partial x_l}}-2\nu\overline{\left(\frac{\partial^2 u'_i}{\partial x_k \partial x_l}\right)^2}$$

$\Downarrow P^{1}\varepsilon \quad \Downarrow P^{2}\varepsilon \quad \Downarrow P^{3}\varepsilon \quad \Downarrow P^{4}\varepsilon \quad \Downarrow Y$

An equation for ε is derived by multiplying the *k* equation by (ε/*k*) and introducing model constants.

$$\nu_t=C_\nu\frac{k^2}{\varepsilon}$$

$$\frac{\partial \varepsilon}{\partial \tau}+\frac{\partial U_j \varepsilon}{\partial x_j}=\frac{\partial}{\partial x_j}\left[\left(\nu+\frac{\nu_t}{\sigma_k}\right)\frac{\partial \varepsilon}{\partial x_j}\right]+C_{z1}P\frac{\varepsilon}{K}-C_{z2}\rho\frac{\varepsilon^2}{K} \qquad (4)$$

$$P=\nu_t\left(\frac{\partial U_i}{\partial x_j}+\frac{\partial U_j}{\partial x_i}\right)\frac{\partial U_j}{\partial x_i}$$

Empirically coefficients

$$\sigma_k=1 \quad C_{z2}=1.92 \quad C_{z1}=1.44 \quad C_\nu=0.09 \quad \sigma_z=1.33$$

The present study is performed with the help a CFD computer program (FLUENT 15.0). is a general purpose computer program using a finite volume method. Navier-Stokes equations written in a rotating, cylindrical frame of references are solved, with rotating domain technique , see Fig. 3.

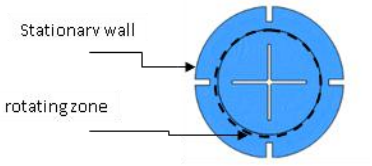

Figure 3: The technique of rotating domain

VALIDATION

To verify the reliability of our simulations and the conformity of our results, they are compared with previous experimental work via (LDV) on a tank of diameter D = 0.490m equipped with a four-blades impeller of size d = 0.245m [K. Suzukawa, S. Mochizuki, H. Osaka. Elsevier. 2006].

The present work is validated according to the global parameter Np which is the number of power by choosing Numbers of Re (0,4 ; 0,7 ; 1 , 1,4 and 1,7) $x10^5$ a good agreement is demonstrated and is clearly confirmed , As shown in Fig.4.

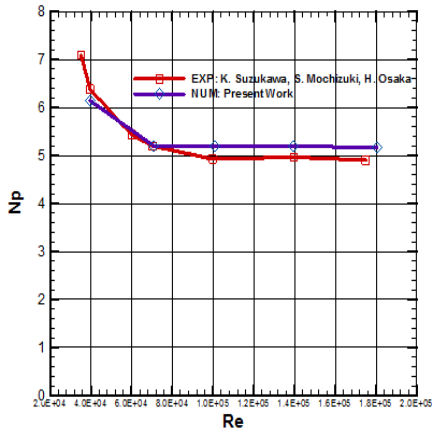

Figure 4: Np at function of Re

RESULTS

For all our simulations we chose a Re = $1.8x10^5$, then we analyzed the influence of the configuration of the baffles, namely baffles (square, circular, rectangular and trapezoidal) on the variation of the local magnitude (the tangential and Radial velocity), on the Vtg vectors, the stream function , on the evolution of the power Np (energy consumption), on the evolution of the turbulent kinetic energy and on the turbulent dissipation rate, the results are The following :

The Tangential Velocity :

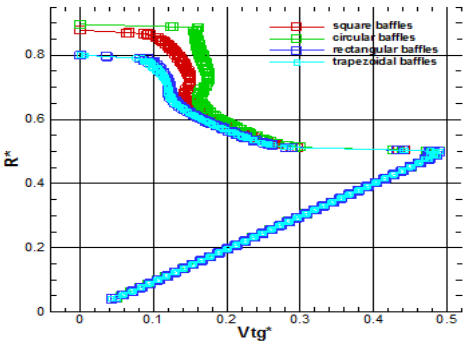

Figure 5: Vtg* on blade and extension

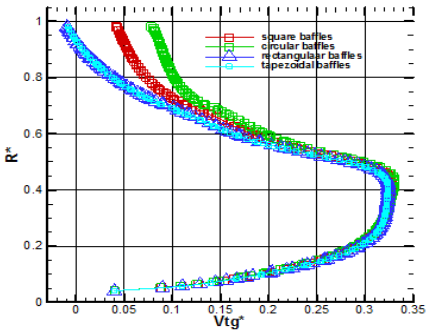

Figure 6: Vtg* on mediator

The Vtg* on blade and extension:

The figure shows that the curves have the same starting point but not the same ending one.

The curves are split into two parts.

1. The first part is a linearity and grows up to the tip of the blade reaching a vertex being the maximum value of Vtg* = 0.5

2. The second part is decreased up to the baffle and wall .

2.1. A rapid decay of the Vtg from the value Vtg*= 0.5 to a value of 0.3 on the same level of the radius R * = 0.5.

2.2. Then from this point (Vtg = 0.3 and R * = 0.5) which is the boundary of the rotating domain, the curves diverge to the baffles and the wall where adhesion (Vtg = 0) occurs, with a different magnitude Of the Vtg, the most important is at the level of the circular baffles, followed by the square baffles, then the rectangular and trapezoidal ones which are almost superimposed, these findings are confirmed by the Fig.8 of the Vtg fields showing the stagnant zones (vortexes) braking in somewhat the flow, they are important at the level of the trapezoidal baffles, rectangular with a less degree for square ones and nonexistent for the circular baffles, also another

confirmation at the level of the contours of the Vtg for the different configurations

The Vtg on mediator:

The curves have the same starting point but not the same ending one.

The velocity profile with a parabolic shape, reaching local summits on the order of 0.34 for the circular baffles, 0.33 for the squares, and 0.32 for the other types, then from the R * = 0.6 (rotating domain boundary) A less rapid decrease of the Vtg for the circular baffles to a value of 0.08, and more and more important for the square ones for a value of 0.04 and the other forms up to the wall with a zero value.

V.2. The radial velocity

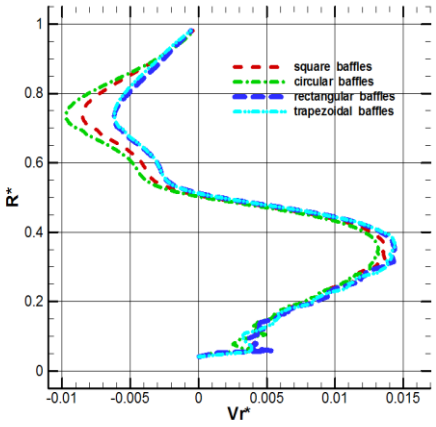

Figure 7: Vr* on mediator

The curves have the same starting point and the same point of arrival.

There are 02 gaits separated by the boundaries of the rotating domain.

2.1 The first is a parabolic form with the largest local summits in the order of 0.014 for the trapezoidal and rectangular baffles, and lower values from 0.013 for the squares to the lower values of 0.012 for the circular baffles.

2.2 the gaits is almost parabolic with the same evolution of the Vr the most important values are for trapezoidal and rectangular baffles up to the smallest value for circular baffles.

The presence of negative velocities is explained with the aspiration of the fluid..

Note ;

by comparing the Vr curves of the baffled and no-baffled tanks,it is found that at the level of a non-baffled tank the value of the Vr is less important Fig.8., Which confirms the notion that the baffles favour the radial and axial flow with respect to the tangential.

The baffles effectively cut the large central vortex observed in the non-baffled mixing tanks Fig.8. The local vortices are formed behind the counter blades**.**

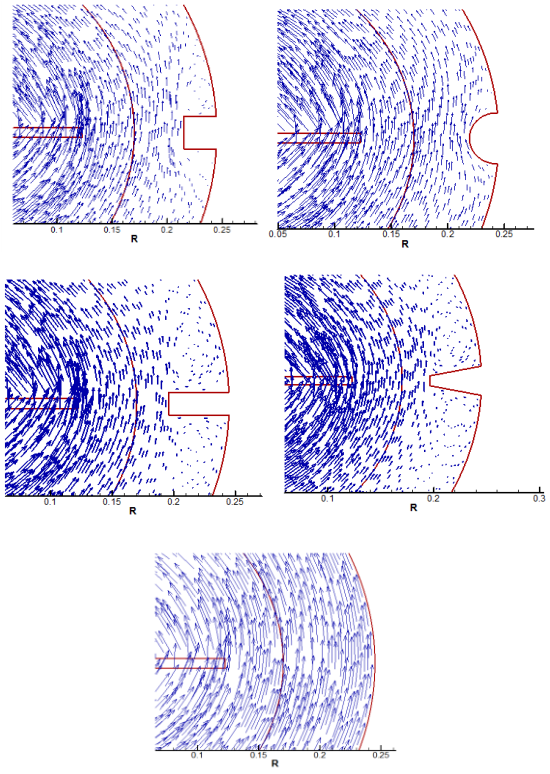

Fig.8. he velocity field for the 4 configuration and the non-baffled tank

THE STREAM FUNCTION

We have analyzed the distribution of the maximum value of the stream function for the four baffle configurations, and we find that it is a decreasing function, the flow rate is less important in the baffle classification (Trapezoidal, rectangular, square and circular), the lowest flow is at the level of the circular baffles, result confirmed by the Np curve for the 4 forms of baffles, Fig 10.

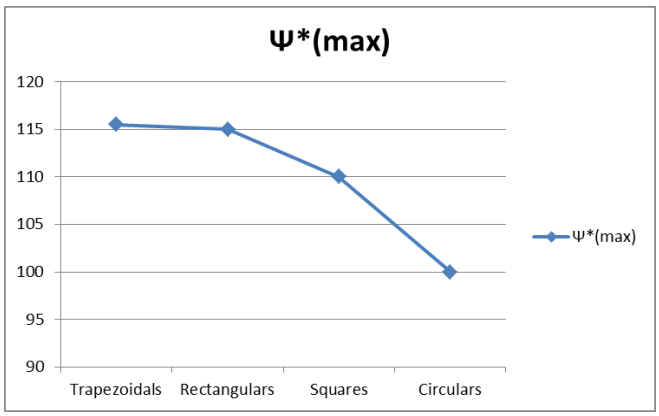

Figure 9 : Ψ*max For the four shapes of baffles

The Energy Consumption

We have studied the evolution of the Np with respect to the four (4) types of baffles, according to the Fig.10, the circular baffles which consume the least energy, the result confirmed by the vector fields of Vtg Fig.8 due to the absence of Vortex (stagnant zone) at these latters with respect to the other forms, meaning that the flow is not braked, And that the transition of the mixture is more fluid and consequently there is no need for a high energy input.

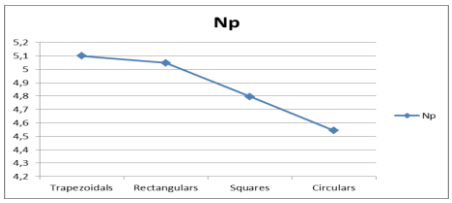

Figure 10: Np max For the four shapes of baffles

THE TURBULENT KINETIC ENERGY (Tke*)

The evolution of the Tke, for the four configurations of baffles.

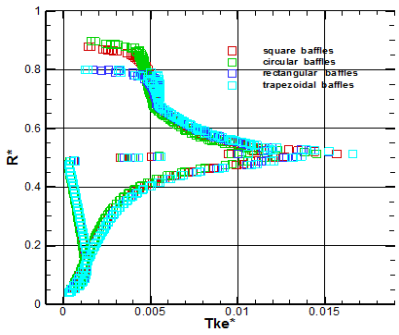

Figure 11: Tke* on blade and extension

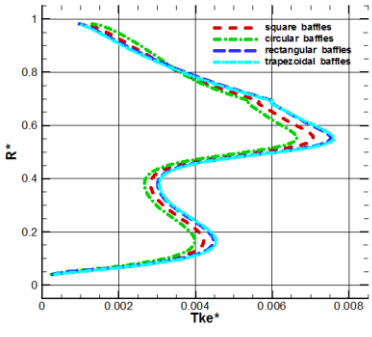

Figure 12: Tke* on mediator

Evolution of Tke * on blade and extension :

The curves have the same starting point but different ending ones, they are split into 2 parts
The Max value of the Tke is at the end of the blades and then decreases to the lowest values near the baffles and the wall, the result confirmed by the contours of the Tke Fig.14.

1.1 **:** the first part of the superimposed curves starting from a zero Tke * at the beginning of the blade, then grows up to the Max value of the Tke * which corresponds to the position of R * = 0.5, with The following results:

Table 2: LES valeurs DE TKE* MAX

Types of baffles	trapezoidal	rectangular	square	circular
Tke* Max	0.0175	0.017	0.016	0.0145

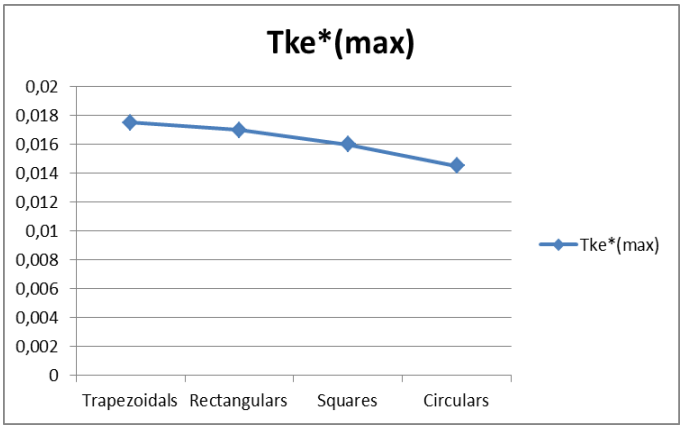

Figure 3: Tke* max For the four shapes of baffles

By comparing the four geometry of baffles, the Max value of Tke corresponds to the trapezoidal ones, and this follows the existence of important vortex behind these baffles Fig.8 field Vtg, which has generated the increase of the turbulent kinetic energy (The vortex intensity) in the fluid favoring its transfer to the small vortices where it dissipates in the form of heat by the forces of viscosity, it is the vortices which dissipate the energy.

The lowest value of Tke is at the level of the circular baffles (no vortices) Fig.8 field vectors Vtg.

1.2 The second part of the curves is a decay of Tke in a manner almost superimposed to R * = 0.8, then a rapid decrease to the trapezoidal and rectangular baffles, as opposed to circular and square baffles to reach Value of Tke * Min = 0.001.

Evolution of Tke* on mediator:

The curves have the same starting point and arrival point, they have a rapid increasing tendency superimposed up to R * = 0.18, then a regression with Tke * Max values for the trapezoidal, rectangular and then square baffles and the Tke * Min for circulars up to R * = 0.4, then a rapid progression similar to the first one, then a decrease similar to the first one to point R * = 0.8 (rotating domain boundary), then a decrease of Tke * minus Fast respectively for circular, square, rectangular and trapezoidal baffles towards the Tke * Min = 0.001

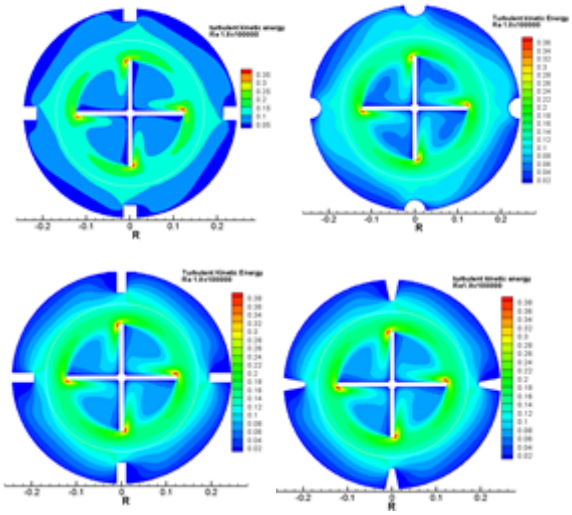

Figure 14: Contours of Tke

THE TURBULENT DISSIPATION RATE (ε*)

The variation of (ε *) for the four types of baffles

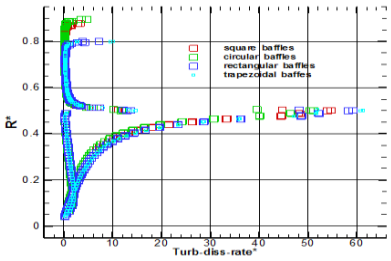

Figure 15: ε* on blade and extension

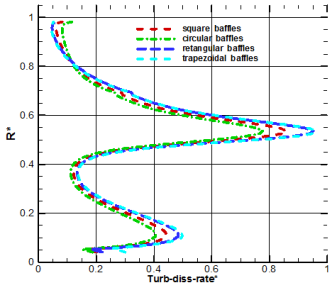

Figure 16: ε* on mediator

Evolution of the ε* on blade and extension:

The curves have the same starting point but different at ending ones, they are split into 2 parts The Max value of the ε * is at the level of the blade tip, then decreases to the lowest values near the baffles and the wall.

1.1 . It is the same evolution as the turbulent kinetic energy. The first part of the superimposed curves starting from a ε * null at the beginning of the blade, then grows to the Max value of the ε * which corresponds to the position of R * = 0.5, with the following results:

Table 3: LES valeurs DE ε* MAX

Types of baffles	trapezoidal	rectangular	square	circular
ε* Max	64	60	55	50

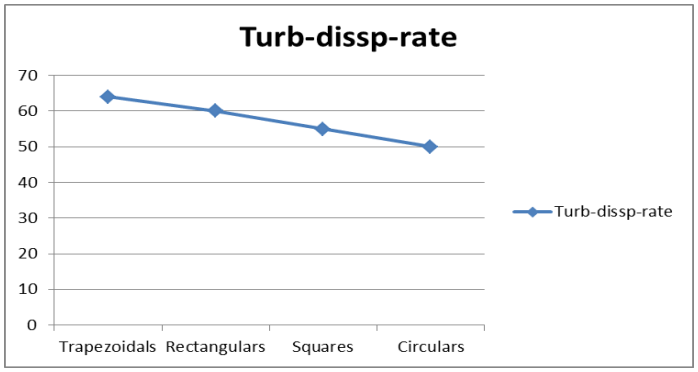

Figure 17: Turb-diss-rate max For the four shapes of baffles

The lowest value of ε * is at the level of the circular baffles (absence of vortex behind the baffle) Fig.8 field Vtg.

1.2 In the second part, the curves are superimposed with a rapid decrease of ε * (horizontally) to R * = 0.5 for a ε * zero along the R * (0.5 to 0.8), then to the wall one Rapid increase for baffles trapeze and rectangle with a ε * = 10.

Unlike square and circular baffles with a ε * = 5

Evolution of ε* on mediator :

The curves have the same appearance and the same interpretations as that of the Tke* on mediator.

CONCLUSION

This study is a form of participation which aimed at reducing the difficulties encountered in the field of mechanical agitation, particularly in the industrial, agro-food, chemical, ect……

A 2D simulation was undertaken by studying the effect of the geometry of baffles on hydrodynamics and energy consumption in an agitated tank by a four-blade impeller in order to have a homogeneous mixture with energy consumption and mixing time reduced.

It has been demonstrated that the circular shape of baffles consumes less energy (reduced Np), and also the circular baffles do not harbor vortex , so optimal dispersion of the mixture, its turbulent kinetic energy and its rate of turbulent dissipation are reduced and compared to the other proposed configurations such as square, rectangular and trapezoidal baffles.
The results provide direction towards optimal design of mixing equipment.

ACKNOWLEDGEMENTS

The authors wish to thank the support of the laboratory ENERGARID of energy in areas with wrinkles , University of Bechar Algeria.

NOMENCLATURE

d	Diameter of the agitator
D	Diameter of the tank
DRD	Diameter of rotating domain
Sb	Surface of baffles
ds	Shaft diameter
Tb	thickness blade
Np	Number of power
P	Power agitation
U,V	Speed Cartesian velocity
Vtg*	Dimensionless Tangential Velocity
Vr*	Dimensionless Radial velocity
X, Y	Cartesian coordinates dimensionless
R^*	Dimensionless radius of the vessel
x, y	Cartesian coordinates dimensional
Tke*	Dimensionless turbulent kinetic energy
θ	Angular position
ε	Turbulente dissipation rate
t	Time
N	Rotational speed
D	Diffusion coefficient
k	Turbulent kinetic energy
p	Pressure
P'	Pressure fluctuation [Pa]
u_i	Velocity component [$m.s^{-1}$]
u'_I	Fluctuation of the velocity
u^+	Velocity of the boundary layer
u_τ	Velocity characteristic of friction
τ_w	Constraint Ranking

Greek symbols

ψ^*	Dimensionless Stream function
ν	Kinematic viscosity of the fluid
ρ	Density of the fluid
μ	Dynamic viscosity of the fluid
ε*	turbulent dissipation rate

Dimensionless numbers

$N_P = \frac{P}{\rho N^3 d^5}$ Number of power

$\mathrm{Re} = \frac{d^2 N \rho}{\mu}$ REYNOLDS NUMBER

REFERENCES

[1] Gramann, P., J., Ph.D. *Thesis, University of Wisconsin-Madison, (1995)*

[2] Yu C., Gunasekaran, S., J. *Food Eng., 71, 2005, p. 295*

[3] Hiraoka, S., Yamada, I., J. *Chem. Eng Japan, 11, 1978, p.487*

[4] Lindley, J.A., J. Agric. *Eng. Research, 8, 1991, p.153*

[5] Takahashi, K., Arai, K., & Saito, S., J. *Chem. Eng. Japan, 13, 1980, p.147*

[6] Aubin, J., Naude, I., Xuereb, C., & Bertrand, J., *Trans. Inst.Chem. Eng., 78A, 2000, p.1105*

[7] Brito-DE LA Fuente, E., Choplin, L., Tanguy, P.A., *Trans. Inst. Chem. Eng. 75A, 1997, p.45*

[8] Anne-Archard, D., BOISSON H., *Intl. Num. Meth. Fluids, 21, 1995, p.75*

[9] Oldshue J.Y. (1983). Fluid Mixing Technology, p. 15. *McGraw Hill, New York.*

[10] Montante G., Lee K., Brucato C.A. and Yianneskis M. (2001). *Numerical simulations of the dependency of flow pattern on impeller clearance in stirred vessels. Chem. Eng. Sci. 56, 3751–3770.*

[11] BujalskiW., Jaworski Z. and NienowW. (2002). *CFD study of homogenization with dual Rushton turbine – comparison with experimental results II: the multiple frame of reference. Trans. Inst. Chem. Eng. 80A, 97–104*.

[12] Marchisio D.L. (2009). *Large eddy simulation of mixing and reaction in a confined impinging jets reactor. Comput. Chem. Eng. 33(2), 408–420.*

[13] Mavros P., Mann R., Vlaer S.D. and Bertr J. (2001). *Experimental visualization and CFD simulation of flow patterns induced by a novel energy-saving dual configuration impeller in stirred vessels. Trans. Inst. Chem. Eng. 78A, 857–866.*

[14] Nienow A.W. (1997). *On impeller circulation and mixing effectiveness in the turbulent flow regime. Chem. Eng. Sci. 52, 2557–2565.*

[15] Sharma R.N. and Shaikh A.A. (2003). *Solids suspension in stirred tanks with pitched blade turbines. Chem. Eng. Sci. 58, 2123–2140.*

[16] Pinelli D. and Magelli F. *(2000). Analysis of the fluid dynamic behaviour of the liquid and gas phases in reactors stirred with multiple hydrofoil impellers. Ind.Eng. Chem. Res. 39(9), 3202–3211*.

[17] Oldshue J.Y. (1983). *Fluid Mixing Technology, p. 15. McGraw Hill, New York.*

[18] Ochieng A., Onyango M.S., Kumar A., Kiriamiti H.K. and Musonge P. *(2008).*

[19] R. Zadghaffari, J.S. Moghaddas and J. Revstedt, *Large eddy simulation of turbulent flow in a stirred tank driven by a Rushton turbine, Comput Fluids, 39 (2010) 1183-1190.*

[20] Bakker, A., Oshinowo, L.M. and Marshall, E.M. (2000) *The Use of Large Eddy Simulation to Eddy Simulation to Study Stirred Vessel Hydrodynamics. Proceeding of the 10th European Conference on Mixing, Delft, 2-5 July 2000, 247-254.*

[21] R. Zadghaffari et all, *A Study on Liquid-liquid Mixing in a stirred tank with a 6-blade Rushton Turbine, Iranian Journal of Chemical Engineering Vol.5, N°. 4, 2008*

[22] Lu,W-M,H-Z .Wu and M-Y *Effects of baffle design on the liquidmixing in an aerated stirred tank with standard Rushton turbine impellers. Chimical Engineering Science,1997.52(21-22):p3843-3851*.

[23] K. Suzukawa, S. Mochizuki, H. Osaka *Effect of the attack angle on the roll and trailing vortex structures in an agitated vessel with a paddle impeller*. *Chemical Engineering Science 61 (2006) 2791–2798*